Adsorption 9: 205–212, 2003

Diffusion of Paraffins in Dealuminated Y Mesoporous Molecular Sieve

CÉLIO L. CAVALCANTE JR.* AND NEUMA M. SILVA
Universidade Federal do Ceará, Dept. Engenharia Química, GPSA-Grupo de Pesquisas em Separações por Adsorção, Campus do Pici, Bl. 709, 60.455-760, Fortaleza, CE, Brazil
celio@ufc.br

EDUARDO F. SOUZA-AGUIAR
Petrobras/Cenpes, Ilha do Fundao, Rio de Janeiro, RJ, Brazil

ELEDIR V. SOBRINHO
Universidade Salvador, Dept. Engenharia, Salvador, BA, Brazil

Abstract. Mesoporous materials have been intensely studied recently, mainly as possible component for FCC (Fluid Catalytic Cracking) catalysts due to their large surface area and accessibility to large hydrocarbon molecules. It is thus of interest for the oil industry to understand the diffusion behavior of some standard molecules in these materials. Y Zeolites, usually employed in fluid catalytic cracking, can be modified by removal of aluminum atoms from the zeolitic framework to present a greater mesoporous contribution. Dealumination of Y zeolite framework is also known to improve the stability of the catalyst thus making it more suitable for the FCC operation. This study presents diffusion measurements performed with the ZLC (Zero-Length Column) method, developed in the late eighties by Eic and Ruthven (1988a, b). The ZLC method has been largely used for a number of systems, either in gas or in liquid phases. We have now applied the ZLC method for gas phase diffusion measurements of linear paraffins (C_7–C_{10}) in dealuminated Y zeolite (USY). Experimental data were obtained at different temperatures (150 to 240°C) and flow rates (40 to 120 ml/min) and correlated through a transient Fickian diffusion model.

Keywords: diffusion, mesoporous molecular sieve, Y zeolite, ZLC—Zero Length Column

Introduction

Catalysts for Fluid Catalytic Cracking (FCC) processes have been increasingly demanded to present enhanced thermal and hydrothermal stabilities as well as selectivity towards products of molecular weight in the range C_7–C_{12}, which have better commercial value. This can be accomplished by removal of aluminum atoms from the Y zeolite framework, thus modifying their crystal structure with formation of mesoporosity and later acid lixiviation to remove extra-framework aluminum (Sobrinho, 1993). These framework modifications may cause changes in both catalyst selectivity and activity. Particularly for Y zeolite, its dealumination may also improve the mobility of larger molecules in the crystal structure, specially for those compounds between C_7 to C_{12}.

This study evaluated diffusivities of n-C_7, n-C_8 and n-C_{10} in dealuminated Y zeolite using the ZLC (Zero-Length Column) method proposed by Eic and Ruthven in the late eighties (1988a, b). The ZLC method has the advantage of minimizing external heat and mass transfer effects in measuring intracrystalline diffusion coefficients.

*To whom correspondence should be addressed.

Table 1. Properties of dealuminated USY zeolite.

Surface Si/Al ratio	1.6
Overall Si/Al ratio	2.8
Framework Si/Al ration	5.4
BET surface area	655 cm^2/g
Micropores volume	0.288 cm^3/g
Mesopores volume	0.077 cm^3/g
Average mesopore size	7 nm
Crystal average radius	0.39 μm
Cluster average radius	12.5 μm

Experimental

The USY mesoporous dealuminated zeolite was obtained from a NaY sample that was submitted to ion exchange with NH_4^+, followed by thermal decomposition between 300 and 400°C and subsequent hydrothermal treatment at 600°C for removal of aluminum atoms from the Al—O—Si bonds. Table 1 shows the properties of the USY zeolite and SEM micrographs are shown in Fig. 1.

The ZLC method was used, as proposed by Eic and Ruthven (1988a). The method consists in following the sorbate desorption from a sample of the zeolite that had been pre-equilibrated with the sorbate at a given temperature, at high flow rate of a inert gas (He or N_2). If the flow rate is sufficiently high, desorption is completely controlled by intracrystalline diffusion, and the sorbate concentration at the outlet of ZLC may be conveniently followed using a typical gas chromatograph flame ionization detector. The experimental setup is shown schematically in Fig. 2. Eic and Ruthven (1988a) applied this method for aromatics diffusion in NaX crystals and for linear paraffins and cyclohexane in 13X and 5A zeolite crystals (Eic and Ruthven, 1988b). Since then, the ZLC method has been studied and applied for a number of zeolite crystal systems (Voogd et al., 1991; Ruthven et al., 1991; Hufton et al., 1994; Cavalcante Jr. et al., 1995; Brandani and Ruthven, 1996a, b; Brandani et al., 2000) and zeolite pelletized systems (Ruthven and Xu, 1993; Brandani, 1996; Silva and Rodrigues, 1996; Brandani et al., 1998).

Mathematical Model

The ZLC model, for spherical particles in isothermal conditions and linear equilibrium isotherm, is shown

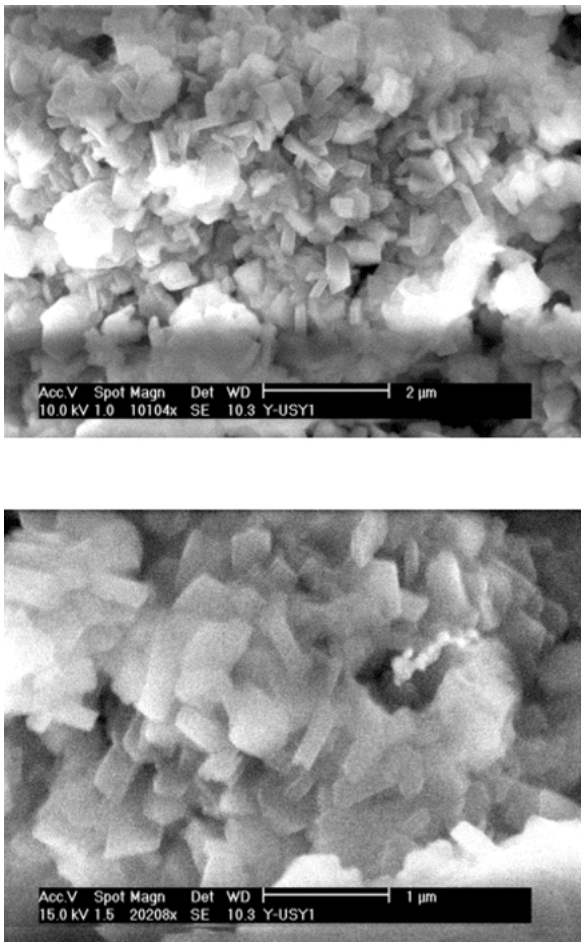

Figure 1. SEM micrographs of USY sample.

in Eqs. (1) (column mass balance) and (2) (adsorbent crystal balance):

$$V_s \frac{d\bar{q}(t)}{dt} + V_f \frac{dC(t)}{dt} + F \cdot C(t) = 0 \tag{1}$$

$$\frac{\partial q(r,t)}{\partial t} = D_c \cdot \left[\frac{\partial^2 q(r,t)}{\partial r^2} + \frac{2}{r} \cdot \frac{\partial q(r,t)}{\partial r} \right] \tag{2}$$

Initial and boundary conditions are:

$$q(r,0) = q_o = K \cdot C_0 = K \cdot C(0) \tag{3}$$

$$\frac{\partial q(0,t)}{\partial r} = 0 \tag{4}$$

$$D_c \frac{\partial q(r_c,t)}{\partial r} + \frac{V_f r_c}{3KV_s} \cdot \frac{\partial q(r_c,t)}{\partial t} + \frac{F r_c}{3KV_s} \cdot q(r_c,t) = 0 \tag{5}$$

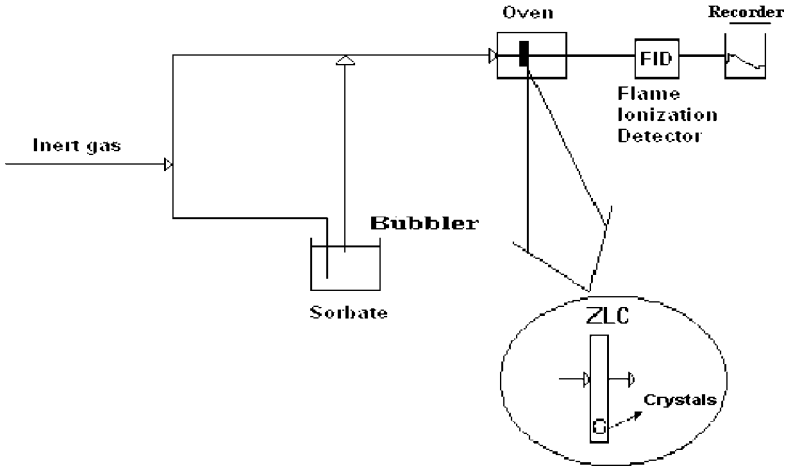

Figure 2. ZLC experimental setup.

Brandani and Ruthven (1995) presented an analytical solution for the model, as shown in Eqs. (6)–(8).

$$\frac{C(t)}{C_0} = 2L \sum_{n=1}^{\infty} \left\{ \frac{\exp\left(-\beta_n^2 D_c t / r_c^2\right)}{\left[\beta_n^2 + \left(1 - L + \gamma\beta_n^2\right)^2 + L - 1 + \gamma\beta_n^2\right]} \right\} \tag{6}$$

$$\gamma = \frac{1}{3}\frac{V_f}{K V_s} \tag{7}$$

$$L = \frac{1}{3}\frac{F}{K V_s}\frac{r_c^2}{D_c} \quad \text{and} \quad \beta_n \operatorname{cotg}(\beta_n) + L - 1 - \gamma\beta_n^2 = 0 \tag{8a, b}$$

In this study, the experimental runs will be analysed following three different approaches: Long Time, Short Time and Method of Moments.

Long Time Analysis

For long times, only the first term of the series in Eq. (6) is significant, so that equation may be rewritten as:

$$\operatorname{Ln}\left(\frac{C}{C_0}\right) = \operatorname{Ln}\left[\frac{2L}{\beta_1^2 + \left(1 - L + \gamma\beta_1^2\right)^2 + L - 1 + \gamma\beta_1^2}\right] - \frac{\beta_1^2 D_c}{r_c^2} t \tag{9}$$

It may be observed that a plot of C/C_0 versus time in a semilog scale will yield in the long time asymptote an estimate for the diffusivity value.

Short Time Analysis

Brandani and Ruthven (1996a) presented a solution for the short time desorption data:

$$\frac{C}{C_0} = 1 - 2L\sqrt{\frac{D}{\pi R^2}} \cdot t^{-1/2} \tag{10}$$

According to Eq. (10), a plot of C/C_0 versus the square root of 1/time will yield an estimate for the diffusivity value. This solution can also be used to evaluate the main diffusional path in the crystalline structure (isotropic or anisotropic diffusion), as shown by Cavalcante Jr. et al. (1997).

Moments Analysis

Brandani and Ruthven (1996b) proposed the use of the moments analysis of the ZLC curves for estimation of the diffusion coefficients. The first and second moments are estimated according to Eqs. (11a) and (11b), respectively:

$$\psi = \frac{\int_o^\infty t \cdot C(t)\,dt}{\int_o^\infty C(t)\,dt} \tag{11a}$$

$$\omega^2 = \frac{\int_o^\infty (t-\psi)^2 \cdot C(t)\,dt}{\int_o^\infty C(t)\,dt} = \frac{\int_o^\infty t^2 \cdot C(t)\,dt}{\int_o^\infty C(t)\,dt} - \psi^2 \tag{11b}$$

The moments are related to the system parameters by Eqs. (12) and (13), from which the diffusion coefficients may be estimated:

$$\psi = \frac{1}{3}\frac{r_c^2}{D_c}\left(\frac{1+3\gamma}{L} + \frac{1}{5}\frac{1}{1+3\gamma}\right) \tag{12}$$

$$\omega^2 = \frac{1}{9}\left(\frac{r_c^2}{D_c}\right)^2\left[\left(\frac{1+3\gamma}{L}\right)^2 + \frac{2}{5}\frac{1}{L} + \frac{13+60\gamma}{175(1+3\gamma)^2}\right] \tag{13}$$

The parameters L and γ may be estimated using Eqs. (14) and (15):

$$\frac{\psi}{\chi} = 1 + \frac{1}{5}\frac{L}{(1+3\gamma)^2} \tag{14}$$

$$\frac{\omega^2}{\varphi^2} = 1 + \frac{6}{7}\frac{(1+10\gamma)L^2}{[L+5(1+3\gamma)^2]^2} \tag{15}$$

where χ is given by:

$$\chi = \int_o^\infty \frac{C(t)}{C_0}dt = \frac{r_c^2}{D_c}\cdot\frac{1+3\gamma}{3L} \tag{16}$$

The moments analysis also allows to discriminate between a diffusion controlled and an equilibrium controlled system, since for the equilibrium control the ratio ω^2/φ^2 is flow rate independent and always equal to unity (Brandani and Ruthven, 1996b).

Results and Discussions

Duplicate runs for the desorption of *n*-decane from USY at 150°C and N_2 flow rate of 40 m/min are shown in Fig. 3. Some runs with different flow rates were also performed in order to evaluate external mass transfer effects and are shown in Figs. 4 and 5. Runs for different linear paraffins with increasing carbon number at same experimental conditions are shown in Fig. 6. Figures 7 and 8 show application of the Long Time and Short Time Analysis to some of our experimental runs.

The Moments Analysis is illustrated in Fig. 9 and the full results, treated as shown by Brandani and Ruthven (1996b), are shown in Table 2 for *n*-C_6 to *n*-C_{10}. It may be observed that all values of ω^2/φ^2 are far from unity, thus confirming absence of external mass transfer resistance in the system studied, as had been previously indicated from the runs using different inert gas flow rates.

A summary of all experimental parameters obtained from the 3 different approaches that were applied to

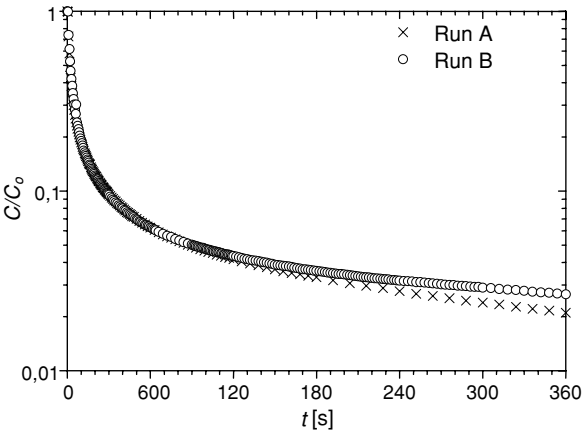

Figure 3. Duplicate desorption runs for *n*-decane from USY zeolite at 150°C. Inert gas flow rate: 40 ml/min of N_2.

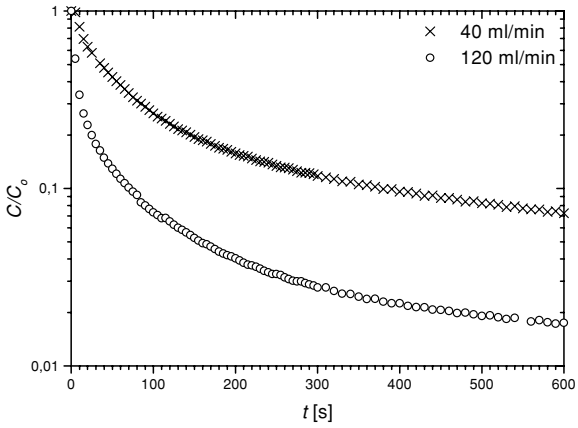

Figure 4. Desorption curves for *n*-octane from USY at 150°C at different flow rates.

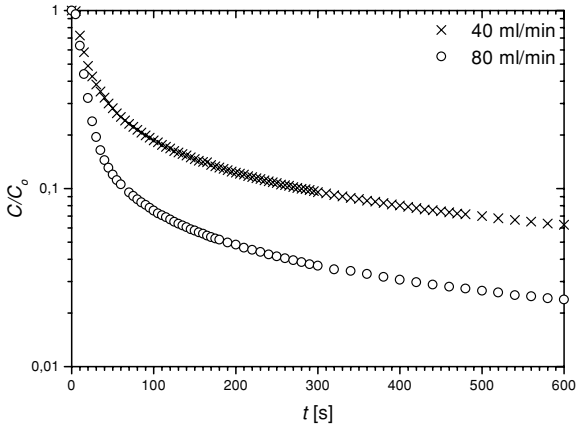

Figure 5. Desorption curves for *n*-decane from USY at 180°C at different flow rates.

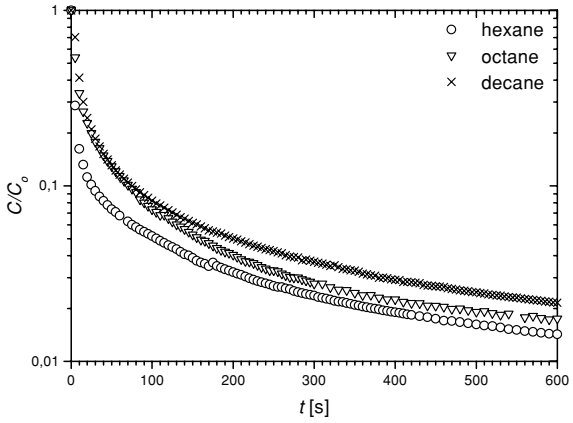

Figure 6. Desorption curves of linear paraffins from USY at 150°C and flow rate of 120 ml/min.

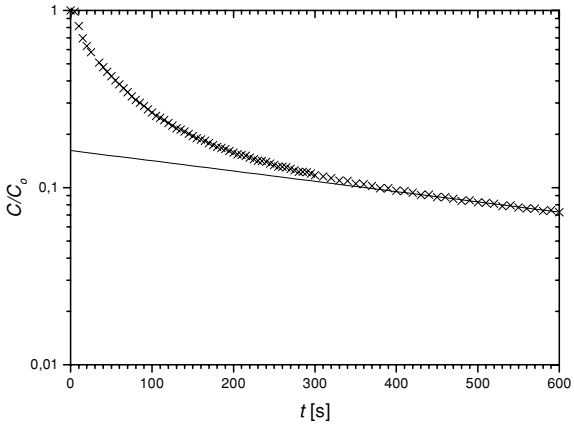

Figure 7. Long Time Analysis for desorption of *n*-octane from USY at 150°C and flow rate of 40 ml/min (straight line represents the long time asymptote).

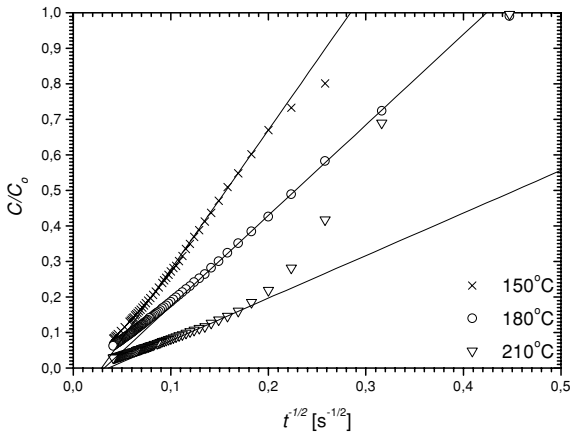

Figure 8. Short Time Analysis for desorption of *n*-heptane from USY at flow rate 30 ml/min. Lines represent the fitting according to Eq. (10).

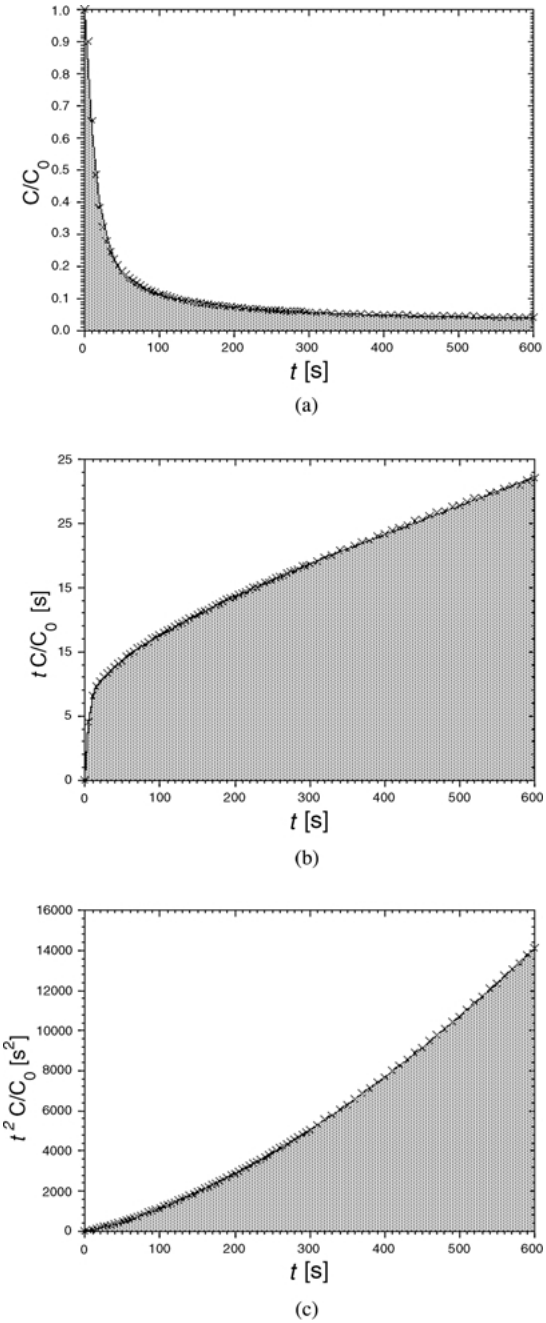

Figure 9. Moments Analysis for desorption of *n*-decane from USY at 210°C and flow rate 40 ml/min. (a) $C/C_0 \times t$; (b) $tC/C_o \times t$; and (c) $t^2C/C_0 \times t$.

our data is shown in Table 3. Reasonable agreement may be observed between the results obtained using the three different approaches, so we decided to take an arithmetic average as an estimate for both D_c/r_c^2 and L. Representation of the fitting of the full data using

Table 2. Results from the moments analysis.

Sorbate	(°C) Temp.	Purge flow rate (ml/min)	φ	ω^2	ω^2/φ^2
n-hexane	150	120	434.1	3.16×10^5	1.68
n-heptane	150	30	651.7	6.46×10^5	1.52
	180		627.1	5.84×10^5	1.49
	210		514.8	4.68×10^5	1.77
n-octane	150	40	567.8	5.02×10^5	1.56
	180		529.4	4.36×10^5	1.55
	150	120	414.9	3.46×10^5	2.01
n-decane	150	40	660.9	7.08×10^5	1.62
	180		739.7	8.23×10^5	1.50
	210		630.9	6.54×10^5	1.64
	150	80	419.5	3.55×10^5	2.02
	180		437.3	3.65×10^5	1.91
	150	120	510.0	4.85×10^5	1.86

the averaged parameters are shown in Fig. 10 for some of the runs.

The blank response of the system for *n*-decane (i.e. an experimental run without adsorbent in the ZLC column) is shown in Fig. 11, along with a typical run at identical conditions of temperature and flow rate (150°C and 80 ml/min). In the blank experiment, C/C_0 decays by two orders of magnitude in about 10 sec,

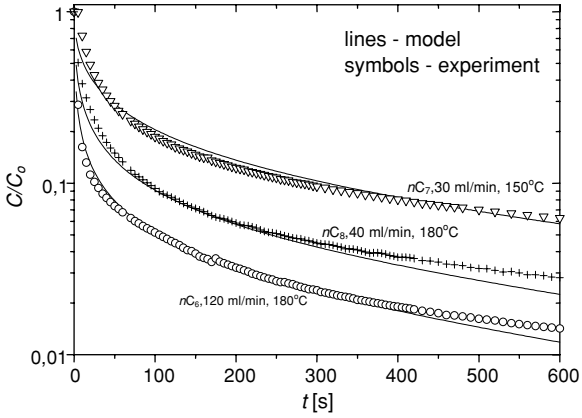

Figure 10. Experimental data and model representation for desorption of *n*-hexane, *n*-heptane and *n*-octane from USY at 150, 180 and 180°C, respectively, at different flow rates.

whereas the typical run shows a very slow concentration decay over a time range of more than 600 sec.

From the diffusivity parameters shown in Table 3, estimates for the activation energy may be obtained, according to Arrhenius equation:

$$D = D^{\mathrm{o}} \exp\left(-\frac{E}{RT}\right) \tag{17}$$

Values obtained for *n*-heptane and *n*-decane were, respectively, 0.8 Kcal/mol and 1.1 Kcal/mol. These

Table 3. Parameters obtained from desorption curves of linear paraffins from USY (D_c/r_c^2 in s^{-1}; L dimensionless; $KV_s/60$ in ml).

Sorbate	T (°C)	F (ml/min)	LTA		STA		MA		Avg		$KV_s/60$
			D_c/r_c^2	L	D_c/r_c^2	L	D_c/r_c^2	L	D_c/r_c^2	L	
n-hexane	150	120	1.76×10^{-4}	56.4	2.00×10^{-4}	71.4	1.66×10^{-4}	63.3	1.80×10^{-4}	63.7	58
n-heptane	150	30	1.42×10^{-4}	12.1	1.91×10^{-4}	11.1	1.43×10^{-4}	12.4	1.59×10^{-4}	11.9	88
	180	30	1.46×10^{-4}	15.5	1.95×10^{-4}	16.7	1.41×10^{-4}	18.0	1.61×10^{-4}	16.7	62
	210	30	1.49×10^{-4}	32.4	2.43×10^{-4}	32.3	1.48×10^{-4}	34.2	1.80×10^{-4}	33.0	28
n-octane	150	40	1.60×10^{-4}	12.7	1.66×10^{-4}	12.5	1.65×10^{-4}	12.3	1.64×10^{-4}	12.5	109
	150	120	1.63×10^{-4}	48.6	1.64×10^{-4}	40.0	1.80×10^{-4}	41.5	1.69×10^{-4}	43.4	91
	180	40	1.69×10^{-4}	14.6	1.74×10^{-4}	15.4	1.66×10^{-4}	15.6	1.70×10^{-4}	15.2	86
n-decane	150	40	1.26×10^{-4}	21.0	2.36×10^{-4}	15.4	1.23×10^{-4}	22.8	1.62×10^{-4}	19.7	69
	150	80	1.62×10^{-4}	27.5	1.48×10^{-4}	20.0	2.00×10^{-4}	19.5	1.70×10^{-4}	22.3	117
	150	120	1.41×10^{-4}	42.0	1.94×10^{-4}	34.5	1.47×10^{-4}	40.7	1.61×10^{-4}	39.1	106
	180	40	1.21×10^{-4}	17.5	1.97×10^{-4}	16.7	1.12×10^{-4}	20.5	1.43×10^{-4}	18.2	85
	180	80	1.65×10^{-4}	35.0	1.92×10^{-4}	31.2	1.75×10^{-4}	33.1	1.77×10^{-4}	33.1	76
	210	40	1.28×10^{-4}	26.4	3.22×10^{-4}	18.9	1.23×10^{-4}	30.2	1.91×10^{-4}	25.1	46

LTA: long time analysis; STA: short time analysis; MA: moments analysis; AVG: arythmetic average.

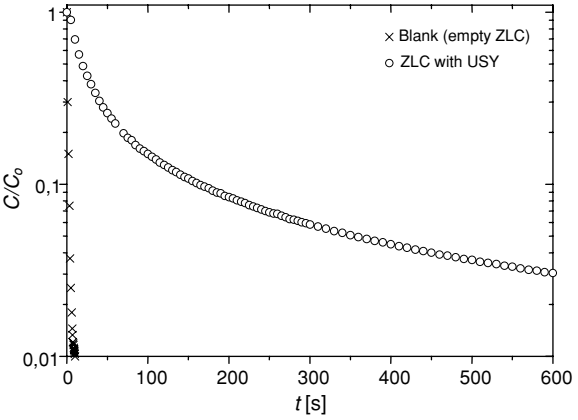

Figure 11. Blank Response of the ZLC system (without USY sample) for desorption of *n*-decane at 150°C and flow rate 80 ml/min (also shown is a typical run at identical conditions for a system containing USY sample).

values are relatively low as compared to regular Y zeolite which may be explained from the opening of the pore structure due to dealumination.

Table 3 also brings a parameter ($KV_s/60$) that may be used to estimate the energy of adsorption for these systems, according to vant Hoff equation:

$$\lim_{C\to 0}\left(\frac{\partial q}{\partial C}\right)_T = K = K^o \cdot e^{-\Delta U^o/RT} \qquad (18)$$

Energies of adsorption were estimated as 7.7 Kcal/mol and 7.3 Kcal/mol for *n*-heptane and *n*-decane, respectively.

As may be seen from Fig. 1, our USY sample consisted of agglomerated clusters (average radius ca. 12.5 μm) of small crystals (average radius ca. 0.4 μm). Diffusivity values, calculated using both the crystal size and the cluster size, are shown in Table 4. Even considering that the diffusional length is the cluster radius, the diffusivity values obtained still seem to be extremely low, compared to other reports from the literature for similar faujasite structure material (NaX crystals, see Table 5). This may be attributed to the protonized nature of the sample of USY that was used, since this is a material to be used in FCC catalysts. The higher acidity of our USY sample (as compared to the acidity of NaX), could probably slow down the diffusion process and be responsible for the large difference in diffusivities that was observed between our USY samples and NaX crystals (as previously reported in Kärger and Ruthven, 1992). This could explain the much lower time constants that were observed in this study, yielding

Table 4. Diffusivity values of linear paraffins in USY. Results are calculated using both the crystals radius (0.39 μm) and the clusters radius (12.5 μm).

			D_c (cm^2/s)	
Sorbate	T (°C)	F (ml/min)	Crystal	Cluster
n-hexane	150	120	2.68×10^{-13}	2.81×10^{-10}
n-heptane	150	30	2.37×10^{-13}	2.48×10^{-10}
	180	30	2.40×10^{-13}	2.53×10^{-10}
	210	30	2.68×10^{-13}	2.81×10^{-10}
n-octane	150	40	2.44×10^{-13}	2.55×10^{-10}
	150	120	2.51×10^{-13}	2.63×10^{-10}
	180	40	2.53×10^{-13}	2.65×10^{-10}
n-decane	150	40	2.41×10^{-13}	2.53×10^{-10}
	150	80	2.53×10^{-13}	2.65×10^{-10}
	150	120	2.39×10^{-13}	2.50×10^{-10}
	180	40	2.13×10^{-13}	2.20×10^{-10}
	180	80	2.63×10^{-13}	2.75×10^{-10}
	210	40	2.84×10^{-13}	2.93×10^{-10}

Table 5. Diffusivity values from this study (USY) compared to NaX crystals diffusivities (from Kärger and Ruthven, 1992).

		D_c (cm^2/s)		
Sorbate	Temp. (°C)	NaX crystals*	USY using crystals radius	USY using clusters radius
n-hexane	150	3.0×10^{-5} (NMR)	2.7×10^{-13}	2.8×10^{-10}
n-heptane	150	2.0×10^{-07} (ZLC)	2.4×10^{-13}	2.5×10^{-10}
n-octane	150	1.0×10^{-5} (NMR)	2.5×10^{-13}	2.6×10^{-10}
n-decane	150	7.0×10^{-8} (ZLC)	2.4×10^{-13}	2.5×10^{-10}

*From Kärger and Ruthven (1992).

such lower apparent diffusivity values for USY samples when compared to typical NaX or Y zeolite crystals.

Conclusions

We have applied the ZLC Method to study the diffusional behavior of linear paraffins in USY zeolites. A Fickian diffusion model, using three different approaches (Long Time Analysis, Short Time Analysis and Moments Methods), provided a good representation of the experimental data. However, our diffusivity values were extremely lower than the values

reported for a similar structure material (NaX crystals). This observation may be due to the high acidic nature of the employed USY samples, which were in the protonized form as used in FCC catalysts. No significant difference in diffusivities was observed between C_6 to C_{10} in the USY sample studied, which may be due to the larger pore opening of the mesoporous structure created by the dealumination of the zeolite Y framework. This might also be the reason for the low activation energies that were estimated from the diffusion results.

Nomenclature

C	Gas phase concentration
C_0	Gas phase concentration at time zero
D	Diffusion coefficient
D_c	Intracrystalline diffusivity
D^o	Pre-exponential factor in Eq. (17)
E	Activation energy
F	Volumetric fluid flow rate
K	Dimensionless Henry's constant
L	Parameter defined in Eq. (8a)
q	Adsorbed phase concentration
$\bar{q}$	Crystal-averaged adsorbed phase concentration
q_o	Adsorbed phase concentration at time zero
$\boldsymbol{R}$	Gas constant
R	Adsorbent particle radius
r	Radial distance
r_c	Crystal (or cluster) radius
T	Temperature
t	Time
$-\Delta U$	Energy of adsorption
V_f	Fluid volume in ZLC
V_s	Adsorbent volume in ZLC
β_n	Roots of Eq. (8b)

Greek Letters

Ψ	First moment
ω	Second moment
γ	Parameter defined in Eq. (7)
χ	Parameter defined in Eq. (16)

Acknowledgments

The authors wish to acknowledge the Department of Analytical Chemistry and Physicochemistry—UFC, the PPGEQ—Chemical Engineering Graduate Program—UFRN and CNPq—Conselho Nacional de Desenvolvimento Cientifico e Tecnologico.

References

Brandani, S., "Analytical Solution for ZLC Desorption Curves with Bi-porous Adsorbent Particles," *Chem. Eng. Sci.*, **51**, 3283–3288 (1996).

Brandani, S., C.L. Cavalcante Jr., A. Guimarães, and D. Ruthven, "Heat Effects in ZLC Experiments," *Adsorption*, **4**, 275–285 (1998).

Brandani, S., M. Jama, and D.M. Ruthven, "Counterdiffusion of p-Xylene/o-Xylene in Silicalite Studied by the Zero-Length Column Technique," *Ind. Eng. Chem. Res.*, **39**, 821–828 (2000).

Brandani, S. and D.M. Ruthven, "Analysis of ZLC Desorption Curves for Liquid Systems," *Chem. Eng. Sci*., **50**(13), 2055–2059 (1995).

Brandani, S. and D.M. Ruthven, "Analysis of ZLC Desorption Curves for Gaseous Systems," *Adsorption*, **2**, 133–143 (1996a).

Brandani, S. and D.M. Ruthven, "Moments Analysis of the Zero Length Column Method," *Ind. Eng. Chem. Res.*, **35**, 315–319 (1996b).

Cavalcante, C.L. Jr., S. Brandani, and D.M. Ruthven, "Evaluation of the Main Diffusion Path in Zeolites from ZLC Desorption Curves," *Zeolites*, **18**, 282–285 (1997).

Cavalcante, C.L. Jr., M. Eic, D.M. Ruthven, and M. Occelli, "Diffusion of *n*-Paraffins in Offretite-Erionite Type Zeolites," *Zeolites*, **15**, 293–307 (1995).

Eic, M. and D.M. Ruthven, "A New Experimental Technique for Measurement of Intracrystalline Diffusivity," *Zeolites*, **8**, 40–45 (1988a).

Eic, M. and D.M. Ruthven, "Diffusion of Linear Paraffins and Cyclohexane in NaX and 5A Zeolite Crystals," *Zeolites*, **8**, 472–478 (1988b).

Hufton, J., S. Brandani, and D.M. Ruthven, "Measurement of Intracrystalline Diffusion by Zero Length Column Tracer Exchange. Studies in Surface Science and Catalysis," in *Proc. 10th Internacional Zeolite Conference*, vol. **84**, pp. 1323–1330, Elsevier, Amsterdam, 1994.

Kärger, J. and D.M. Ruthven, *Diffusion in Zeolites and Other Microporous Solids*. John Wiley & Sons, New York, 1992.

Ruthven, D.M., M. Eic, and E. Richard, "Diffusion of C_8 Aromatic Hydrocarbons in Silicalite," *Zeolites*, **11**, 647–653 (1991).

Ruthven, D.M. and Z. Xu, "Diffusion of Oxygen and Nitrogen in 5A Zeolite Crystals and Commercial 5A Pellets," *Chem. Eng. Sci*., **48**, 3307–3312 (1993).

Silva, J.A.C. and A.E. Rodrigues, "Analysis of ZLC Technique for Diffusivity Measurements in Bidisperse Porous Adsorbent Pellets," *Elsevier*, *Gas. Sep. Purif.*, **10**(4), 207–224 (1996).

Sobrinho, E.V., Preparação e Caracterização da Zeólita Y com Alto Teor de Silício Obtida por Desaluminação em Série. Tese de Mestrado, São Carlos, UFSCar, 1993.

Voogd, P., H. van Bekkum, D. Shavit, and H.W. Kouwenhoven, *J. Chem. Soc. Faraday Trans.*, **87**(21), 3575–3580 (1991).